Mendeleev Communications

Mendeleev Commun., 2025, **35**, 714–716

Hydrogenation of styrene oxide into 2-phenylethanol over nanosized supported copper phyllosilicate catalyst

Elena A. Redina,*[a] Alexandra A. Obraztsova,[b] Igor V. Mishin,[a] Gennady I. Kapustin[a] and Leonid M. Kustov[a]

[a] *N. D. Zelinsky Institute of Organic Chemistry, Russian Academy of Sciences, 119991 Moscow, Russian Federation. E-mail: redinaea@ioc.ac.ru, redinalena@yandex.ru*
[b] *Higher Chemical College of the Russian Academy of Sciences, D. I. Mendeleev University of Chemical Technology of Russia, 1250479 Moscow, Russian Federation*

DOI: 10.71267/mencom.7782

The nanosized supported copper phyllosilicate catalyst demonstrated remarkable effectiveness as a novel system for the hydrogenation of styrene oxide to produce 2-phenylethanol. This study highlights the unique properties of the copper phyllosilicate phase, which enhances the catalytic activity and contributes to the high selectivity to primary alcohol.

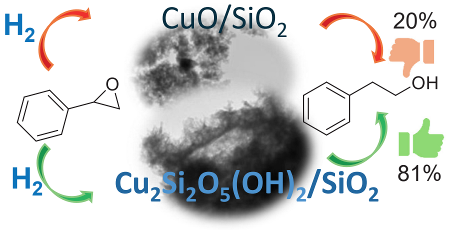

Keywords: primary alcohols, hydrogenation, copper phyllosilicate, heterogeneous catalysis, 2-phenylethanol, styrene oxide.

Primary alcohols are essential substrates in organic synthesis and chemical industry. For example, 2-phenylethanol (PEA) **1** that naturally can be extracted from rose oil is used as a common fragrance.[1] In addition, it possesses an antimicrobial and fungicide activity; therefore, it is applied as a component of antiseptics, deodorants, and cosmetics.[2] The main strategies to obtain PEA **1** consist in the Grignard synthesis using phenylmagnesium halogenides and the Friedel–Crafts alkylation of benzene with ethylene oxide using equimolar amounts of $AlCl_3$ as a Lewis acid. Both of the methods suffer from the need of further product purification, as well as require the use of explosive substrates and special anti-corrosive equipment.[3]

On the other hand, hydrogenation of epoxides is considered as an easy and atom-economical way to obtain anti-Markovnikov primary alcohols from available alkenes.[4] In this regard, PEA **1** was obtained from styrene oxide **2** by heterogeneous hydrogenation over both noble-metal and non-noble metal-based catalysts (Scheme 1).[5–9] Among different non-noble based catalysts used for hydrogenation reactions,[10] copper phyllosilicate is the best candidate. Copper phyllosilicates represents a lamellar chrysocolla structure with a common formula $Cu_2Si_2O_5(OH)_2$ that consists of a SiO_4 tetrahedra layer and a layer of CuO_6 octahedra.[11] The partial thermal decomposition or reduction of copper phyllosilicates indeed leads to the formation of unique materials with enhanced catalytic properties. During this process, isolated fine Cu nanoparticles can be generated, which are well-dispersed within a mesoporous silica support. This configuration not only increases the surface area available for catalytic reactions but also enhances the stability of the copper nanoparticles against sintering and agglomeration. These catalysts are actively used in hydrogenation of carboxylic acids and esters,[12–14] carbonyl compounds,[15] aromatics,[16] and nitro compounds,[17] as well as in hydrodeoxygenation reactions[18] and hydroamination of carbonyls with aromatic nitro compounds.[19] At the same time, phyllosilicates have not yet been applied in hydrogenation of epoxides.

There are several methods for synthesizing copper phyllosilicates, including the ammonia evaporation method,[20] selective adsorption of the copper tetraamine complex,[21] and the deposition–precipitation method utilizing thermal hydrolysis of urea (DPU).[22] Among these, the DPU method is particularly advantageous due to its simplicity and ability to utilize SiO_2 as a silicon source. In this study, we aim to investigate the phase and morphology transformations that occur during the synthesis of supported copper phyllosilicates using the DPU procedure. The resulting catalyst can effectively catalyze the hydrogenation of styrene oxide **2** to produce PEA **1** without requiring any preliminary activation steps.

The supported copper phyllosilicate Cu/SiO_2 (Cu, 12 wt%) was prepared by the DPU procedure from $Cu(NO_3)_2$, urea, and commercial SiO_2 (‘KSKG’) at 92 °C according to the method

Table 1 Structural characteristics of the obtained catalysts.

Entry	Sample	$A_{BET}/m^2\ g^{-1}$	$V_{total}/cm^3\ g^{-1}$	$V_{meso}/cm^3\ g^{-1}$	$V_{micro}/cm^3\ g^{-1}$	$D_{av.\ pore}/nm$
1	SiO_2	100	0.671	0.671	no	27
2	Cu/SiO_2-1h-110	81	0.409	0.409	no	20
3	Cu/SiO_2-4h-110	123	0.560	0.557	0.003	18
4	Cu/SiO_2-8h-110	261	0.614	0.610	0.004	3.5, 17
5	Cu/SiO_2-8h-300	262	0.634	0.628	0.004	3.5, 16
6	Cu/SiO_2-WI	100	0.409	0.409	no	29

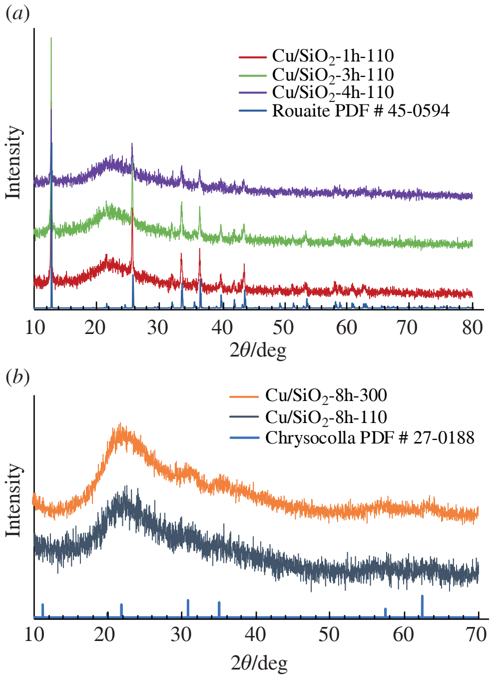

Figure 1 (*a*) XRD pattern of Cu/SiO_2 samples obtained after 1, 3, and 4 h of DPU processing, dried at 110 °C. (*b*) XRD pattern of the Cu/SiO_2 sample obtained after 8 h of DPU processing, dried at 110 °C (Cu/SiO_2-8h-110) and then calcined at 300 °C (Cu/SiO_2-8h-300).

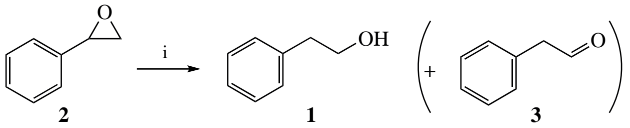

Scheme 1 *Reagents and conditions*: i, styrene oxide **2** (0.4 mmol), catalyst (50 mg), H_2 (10 atm), THF (2.2 ml), 150 °C.

Table 2 Catalytic performance of the obtained samples.[a]

Entry	Sample	*t*/h	Yield of PEA **1** (%)[b]
1	Cu/SiO_2-4-110	9	20
2	Cu/SiO_2-8-110	9	64
3	Cu/SiO_2-8-300	9	81
4	Cu/SiO_2-8-300	5	53
5	Cu/SiO_2-WI	9	20

[a] For condition details, see Scheme 1. [b] ^{1}H NMR yield calculated with the use of $C_2H_2Cl_4$ as an external standard.

described earlier.[19] The 12% Cu/SiO_2 sample was also prepared by the conventional wet impregnation (WI) method (Table 1 and Online Supplementary Materials, Table S1 and Figure S1). During the DPU synthesis, the probe of solid was taken after 1, 3, 4, and 8 h and dried at 110 °C overnight.

The formation of copper phyllosilicate proceeds *via* the preliminary deposition of the $Cu_2(NO_3)OH_3$ rouaite phase [Figure 1(*a*)] onto SiO_2, and it becomes more amorphous in time with the mother liquor pH growth due to urea thermal hydrolysis (see Table S1). Thin plate-shape crystals of rouaite can be recognized from the SEM and TEM micrographs of the samples obtained after 1–4 h of catalyst synthesis [Figure 2(*a*), and Figures S3, S4, parts *a*, *b*]. Similar particles were observed for the rouaite phase obtained from NaOH-hydrolyzed $Cu(NO_3)_2$ with a $NaOH/Cu(NO_3)_2$ ratio of 1–1.5.[23] In the TEM images of the Cu/SiO_2-4h-110 sample, among crystals of 50–100 nm with a monoclinic structure [see Figure 2(*d*)] there are also small particles of 5 nm. After 8 h of the DPU processing, the pH increased to 7 and the rouaite phase completely disappeared because of its dissolution. Two process can proceed at pH > 6 and $T > 90$ °C, which means: (1) water molecules interact with the silica surface, breaking Si–O–Si bonds, and form silanol groups (Si–OH) with the further formation of some amount of silicic acid;[24,25] (2) hydrolyzed copper ions interact with Si–OH to form a $[(HO)_3Si]–O–[Cu(H_2O)_4(OH)]$ species whose polymerization leads to the formation of a poorly crystallized chrysocolla phase,[12] recognized in XRD pattern [see Figure 1(*b*)]. In the SEM and TEM images of the Cu/SiO_2-8h-110 sample, a characteristic net like acicular structure of chrysocolla can be seen [see Figure 2(*b*),(*e*), and Figure S4, part *c*]. Calcination of the sample at 300 °C caused the formation of a more crystalline chrysocolla phase [see Figure 1(*b*)], and net filaments became thinner [see Figure 2(*c*)]. A net of fibers with nanoparticles of 3–4 nm on-top was observed in TEM images of the Cu/SiO_2-8h-300 sample [see Figure 2(*f*)].

The formation of copper phyllosilicate is associated with the development of a secondary porous structure within the SiO_2 pores with enhanced interaction of the Cu-containing phase with SiO_2 (Figure S2), resulting in an increased specific surface area (SSA). Initially, the precipitation of the rouaite phase on the SiO_2 surface and within its pores led to a decrease in both the SSA and pore volume (Table 1, entries 1, 2). As the duration of the DPU synthesis and pH levels increased, thus facilitating the formation of the chrysocolla phase, the SSA began to rise, reaching 261 $m^2 g^{-1}$ for the sample obtained after 8 h (entry 4). Additionally, a significant redistribution of pore sizes was noted. Calcination of the sample at 300 °C did not alter the SSA value; however, it did result in an increase in pore volume (entry 5) due to the formation of a thin fiber network observed by SEM and TEM [Figure 2(*c*),(*f*)].

The prepared catalysts were evaluated for their effectiveness in the hydrogenation of styrene oxide **2** to produce PEA **1** (see Scheme 1), as summarized in Table 2. The presence of the copper phyllosilicate phase significantly enhanced the catalytic activity of the Cu/SiO_2 catalyst. In contrast, the low activity observed for the Cu/SiO_2-WI and Cu/SiO_2-4-110 samples was attributed to their lower specific surface area and the presence of larger crystalline copper-containing phases (see Table S1) inactive in the hydrogenation reaction and the main product was phenylacetaldehyde **3**.

The most impressive yield of 81% for PEA **1** was achieved with the Cu/SiO_2-8-300 catalyst (see Table 2, entry 3). This catalyst exhibited a high SSA and featured small nanoparticles measuring 3–4 nm that were positioned atop thin fibers of copper phyllosilicate. The results indicate that optimizing the catalyst structure can significantly influence its performance in the hydrogenation of epoxides to primary alcohols. The herein obtained nanosized supported copper phyllosilicate catalyst was shown for the first time to be an effective system in styrene oxide **2** hydrogenation to 2-phenylethanol **1**.

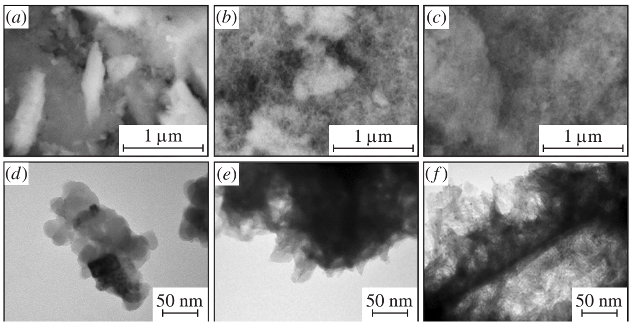

Figure 2 (*a*, *d*) SEM and TEM images of the Cu/SiO_2-4h-110 sample. (*b*, *e*) SEM and TEM images of the Cu/SiO_2-8h-110 sample. (*c*, *f*) SEM and TEM images of the Cu/SiO_2-8h-300 sample.

This work was supported by the Russian Science Foundation (grant no. 24-73-10149). NMR, TEM, and SEM studies were performed in the Shared Research Center of Zelinsky Institute of Organic Chemistry RAS, Moscow.

Online Supplementary Materials

Supplementary data associated with this article can be found in the online version at doi: 10.71267/mencom.7782.

References

1 *Common Fragrance and Flavor Materials: Preparation, Properties and Uses*, 1st edn., eds. H. Surburg and J. Panten, Wiley, 2016; https://doi.org/10.1002/9783527693153.

2 B. D. Mookherjee and R. A. Wilson, in *Kirk-Othmer Encyclopedia of Chemical Technology*, 1st edn., ed. K. Othmer, Wiley, 2000, pp. 483–489; https://doi.org/10.1002/0471238961.0205142613151511.a01.

3 C. Sell, in *Chemistry of Fragrances*, ed. C. S. Sell, Royal Society of Chemistry, 2006, pp. 52–131; https://doi.org/10.1039/9781847555342-00052.

4 S. Thiyagarajan and C. Gunanathan, *Chem. – Asian J.*, 2022, **17**, e202200118; https://doi.org/10.1002/asia.202200118.

5 M. Viswanadhan, A. Potdar, A. Divakaran, M. Badiger and C. Rode, *Res. Chem. Intermed.*, 2016, **42**, 7581; https://doi.org/10.1007/s11164-016-2554-3.

6 E. Thiery, J. Le Bras and J. Muzart, *Green Chem.*, 2007, **9**, 326; https://doi.org/10.1039/B616486B.

7 F. Unglaube, H. Atia, S. Bartling, C. R. Kreyenschulte and E. Mejía, *Helv. Chim. Acta*, 2023, **106**, e202200167; https://doi.org/10.1002/hlca.202200167.

8 A. Sasu, B. Dragoi, A. Ungureanu, S. Royer, E. Dumitriu and V. Hulea, *Catal. Sci. Technol.*, 2016, **6**, 468; https://doi.org/10.1039/c5cy00779h.

9 F. Zaccheria, R. Psaro, N. Ravasio, L. Sordelli and F. Santoro, *Catal. Lett.*, 2011, **141**, 587; https://doi.org/10.1007/s10562-010-0543-5.

10 S. I. Pomogailo, E. G. Chepaikin, O. P. Tkachenko, O. N. Bubelo, R. I. Jussupkaliyeva and L. M. Kustov, *Mendeleev Commun.*, 2025, **35**, 1; https://doi.org/10.71267/mencom.7645.

11 C. J. G. van der Grift, P. A. Elberse, A. Mulder and J. W. Geus, *Appl. Catal.*, 1990, **59**, 275; https://doi.org/10.1016/S0166-9834(00)82204-6.

12 W. Di, J. Cheng, S. Tian, J. Li, J. Chen and Q. Sun, *Appl. Catal. Gen.*, 2016, **510**, 244; https://doi.org/10.1016/j.apcata.2015.10.026.

13 D.-T. To and Y.-C. Lin, *Catalysts*, 2021, **11**, 255; https://doi.org/10.3390/catal11020255.

14 X. Dong, X. Ma, H. Xu and Q. Ge, *Catal. Sci. Technol.*, 2016, **6**, 4151; https://doi.org/10.1039/C5CY01965F.

15 T. Shoosri, S. Thongratkaew, B. Rungtaweevoranit, W. Kraithong, K. Faungnawakij, T. Teerawatananond, T. Sooknoi, S. Kuboon, J. Panpranot and P. Weerachawanasak, *ChemCatChem*, 2025, **17**, e202401661; https://doi.org/10.1002/cctc.202401661.

16 X. Ma, G. Huang, Z. Sun, Y.-Y. Liu, Y. Wang and A. Wang, *ACS Appl. Nano Mater.*, 2023, **6**, 14756; https://doi.org/10.1021/acsanm.3c02180.

17 E. V. Shuvalova and O. A. Kirichenko, *Mendeleev Commun.*, 2021, **31**, 875; https://doi.org/10.1016/j.mencom.2021.11.036.

18 H. Wang, W. Zhao, M. U. Rehman, W. Liu, Y. Xu, H. Huang, S. Wang, Y. Zhao, D. Mei and X. Ma, *ACS Catal.*, 2022, **12**, 4724; https://doi.org/10.1021/acscatal.2c00380.

19 E. Redina, N. Arkhipova, G. Kapustin, O. Kirichenko, I. Mishin and L. Kustov, *ChemCatChem*, 2023, **15**, e202300294; https://doi.org/10.1002/cctc.202300294.

20 J. Gong, H. Yue, Y. Zhao, S. Zhao, L. Zhao, J. Lv, S. Wang and X. Ma, *J. Am. Chem. Soc.*, 2012, **134**, 13922; https://doi.org/10.1021/ja3034153.

21 T. Toupance, M. Kermarec, J.-F. Lambert and C. Louis, *J. Phys. Chem. B*, 2002, **106**, 2277; https://doi.org/10.1021/jp013153x.

22 O. Kirichenko, G. Kapustin, I. Mishin, V. Nissenbaum, E. Shuvalova, E. Redina and L. Kustov, *Molecules*, 2022, **27**, 5147; https://doi.org/10.3390/molecules27165147.

23 C. Henrist, K. Traina, C. Hubert, G. Toussaint, A. Rulmont and R. Cloots, *J. Cryst. Growth*, 2003, **254**, 176; https://doi.org/10.1016/S0022-0248(03)01145-X.

24 B. M. Lowe, C.-K. Skylaris and N. G. Green, *J. Colloid Interface Sci.*, 2015, **451**, 231; https://doi.org/10.1016/j.jcis.2015.01.094.

25 F. K. Crundwell, *ACS Omega*, 2017, **2**, 1116; https://doi.org/10.1021/acsomega.7b00019.

Received: 31st March 2025; Com. 25/7782